Nano World Journal

https://doi.org/10.17756/nwj.2023-111

Research Article

Open Access

Modification of Optical Parameters of Solid Polymer Electrolyte Films for Optoelectronic Device Applications

Sunil Kumar[1,2] and Sannappa J[1*]

[1]*Department of PG Studies and Research in Physics, Jnana Sahyadri, Kuvempu University Shankaraghatta, India*
[2]*Department of Physics, S.S Arts College and T.P Science Institute, Sankeshwar, India*

***Correspondence to:**
Sannappa J
Department of PG Studies and Research in Physics, Jnana Sahyadri, Kuvempu University Shankaraghatta, India
E-mail: Sannappaj2012@gmail.com

Received: October 28, 2022
Accepted: February 17, 2023
Published: February 20, 2023

Citation: Kumar S, Sannappa J. 2023. Modification of Optical Parameters of Solid Polymer Electrolyte Films for Optoelectronic Device Applications. *NanoWorld J* 9(1): 8-14.

Published by United Scientific Group

Abstract

In this work, a time saving, and economical solution cast approach was applied to make solid polymer electrolyte films using hydroxypropyl methylcellulose and sodium bromide. A range of techniques was used to characterize the films, such as Ultraviolet–Visible (UV-Vis) spectroscopy and X-ray diffraction (XRD). The optical factors like refractive index (n), dielectric properties including real and imaginary parts (ε_1 and ε_2), optical conductivity and extinction coefficient were investigated. The absorption edge (E_e) was relocated with increase of salt to a province of lower photonic energy. This caused the rapid decrease of direct and indirect optical bandwidth gaps from 5.59 to 2.57 eV and 4.61 to 2.44 eV. The optical dielectric loss approach was successfully adopted as a stand-in method for determining the optical band gap. The optical dielectric constant variation with change in optical band gap verified Penn's model. The XRD spectra was used to examine the structural variation, the extent of interaction was evidenced by the relatively wide amorphous phase of the hydroxypropyl methylcellulose (HPMC) polymer with an increase of the NaBr salt. Finally, Tauc's approach was used to specify different kinds of electrical transitions within the polymer matrix. The solid polymer electrolyte with an expanded amorphous percentage is key factor for application in optoelectronic devices.

Keywords

Solid polymer electrolyte, Optical band gap, Penn's model, Optical dielectric function, Dielectric loss method

Introduction

Nowadays energy conversion and storage devices generally use solid polymer electrolytes (SPEs). Because they are environmentally friendly, leakage-free, combustion-free, flexible, lightweight, solvent-free, forms films, and importantly it has good ion transport property compared to the liquid ionic solution [1-3]. Moreover, these SPE qualities may be tailored to any desired shape, making them appropriate for mass manufacture. The first SPE was reported based on poly (ethylene oxide) complexed with alkali metal salts in the year 1973 by Fenton et al. [4]. Later, Vashishta et al. [5] showed that ionic conductivity of such complexations could reach 10^{-5} S/cm under room temperature, this promised the development SPEs. Later, a number of studies took place on SPEs showing good results on optical and conductivity parameters. The easy processing and low-cost production of polymer-based optical communications are attracting more attention than silica-based optical materials [6, 7]. Previous research has shown that functional materials and biopolymer composites with appropriate optical band gaps are ideal for optoelectronic devices and organic light-emitting diodes [8-12]. However, one of the most difficult jobs for photovoltaic and optoelectronic applications is

establishing a suitable band gap material [13]. The majority of conjugated polymers are reported to be narrow-band gap polymers. However, conjugated polymers have some disadvantages, such as poor performance and rapid decomposition [14, 15]. Instead, polar polymers such as cellulose and chitosan are relatively inexpensive with good film-forming and long-life properties. The current study used HPMC as a host polymer. Because of its distinct advantages over other cellulose-based polymers. It is thermally stable and forms stable thin films, making it the preferred host polymer. It is frequently used in the biomedical and pharmaceutical fields since it is environmentally safe and non-toxic. In addition to this, nowadays HPMC is used in various industries because it is water soluble and dissolves a variety of metal salts [16, 17]. Here the dopant used is Sodium bromide because recently sodium-based solid polymer electrolytes are attracting more attention than lithium. Because sodium ion is readily available, economic and more moisture resistant than lithium [18-21]. However, the energy density of sodium would not exceed that of lithium, but this is not a significant concern in the sphere of large-scale production, where operating costs and durability are the most essential factors [22, 23].

The optical spectrum is a valuable resource for understanding band structure and optical parameters of polymers [6]. In this work, we incorporated NaBr into an HPMC polymer in order to achieve the desired optical properties. In this report, it is shown that the amorphous segment of HPMC improved, and the optical band gap energy decreased. The solution cast methodology and small optical energy gap show the significance of the current study.

Materials and Methods

The solution cast method was used to make HPMC-based polymer electrolytes. All analytic grade NaBr and HPMC chemicals were furnished from Sigma Aldrich. The pure film was prepared by mixing 3 gm of HPMC powder in 100 ml of triple distilled water (3 wt%) and stirring the liquid for many hours at room temperature with a magnetic stirrer until the HPMC is completely dissolved. Furthermore, NaBr with a suitable weight percentage ratio (0.2 wt%, 0.4 wt%, and 0.8 wt%) was added to each generated 3 wt% (100 ml) of HPMC polymeric solution for 10 - 12 h under constant stirring. After that, solutions were put in a flattened glass slab/petri dish and allowed to evaporate for 5 days. Finally, the film samples were maintained in desiccators for further study.

Following film preparation, samples were tested by XRD and UV-Vis spectroscopy. The structural analysis of the produced polymer film was performed using the Rigaku Miniflex-II X-ray diffractometer with Ni filtered, CuKα radiation (λ = 1.540 Å). A double-beam UV-Vis spectrometer was used to evaluate the optical characteristics of all samples (Lambda 35).

Results and Discussion

Absorption and transmittance study

The addition of NaBr profoundly affected the polymer's optical response. Figure 1 shows absorbance spectra between 200 and 800 nm. The methyl groups n-π* transition might be responsible for the 270 nm absorption band [24-26]. This band is shifted to a higher wavelength and an increase of absorbance takes place with salt concentration due to intermolecular stacking. The intensity of absorption is determined by the number of absorbing molecules. This is in agreement with previous studies and findings [27-30].

Figure 2 shows a transmittance plot. In the visible range,

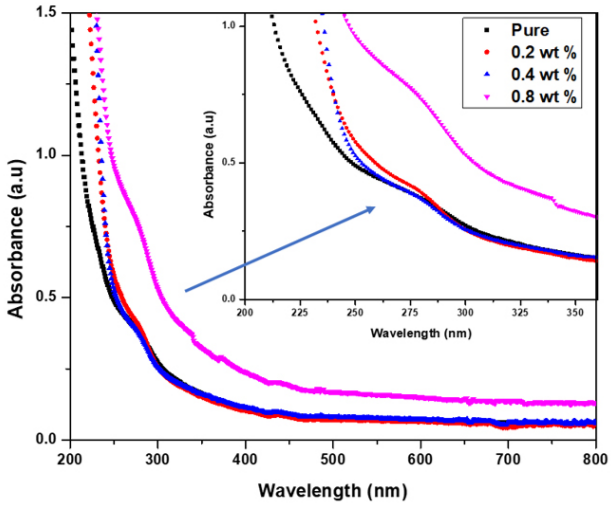

Figure 1: Absorbance spectrum for pure and doped samples.

pure HPMC exhibits accountable transparency of around 90%. HPMC is a transparent polymer [31]. However, increasing the salt content reduces transparency due to changes in the refractive index. This occurs as a result of scattering within the doped layers, which alters the refractive index [32]. However, maintaining the transparency of doped films is challenging. Significantly, the visible range transparency of the doped samples was observed to be greater than 70%.

Refractive index analysis (n)

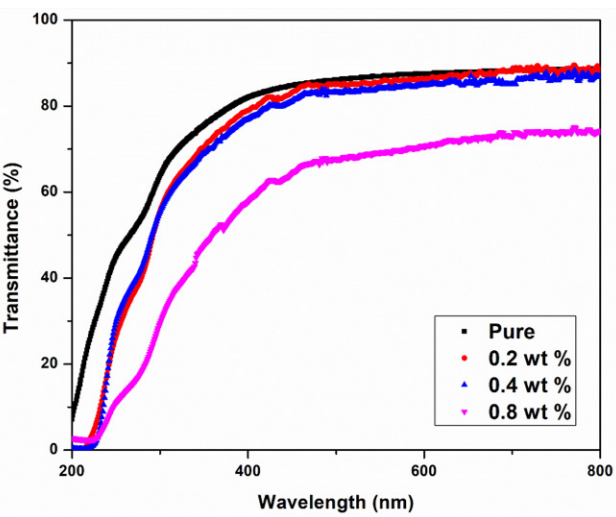

Figure 2: Transmittance spectrum of pure and doped samples.

The optical refractive index (n) of the medium, is one of the crucial parameters that can be obtained by equation (1) [33]. Figure 3 illustrates the proper dispersion behaviour, as

the wavelength rises, the refractive index falls [34]. This dispersion behavior is key for the design of optical systems [32]. In the visible zone, n is non-dispersive and does not equal zero. This alteration in the n value is proof that interactions between photons and electrons are taking place in the films.

$$n = \frac{1}{T_S} + \sqrt{\frac{1}{T_S - 1}} \quad (1)$$

Where, T_S is the percentage transmission coefficient.

The absorption coefficient (α) is obtained by the equation (2) [35].

$$\alpha = \frac{1}{d}\ln\left(\frac{1}{T}\right) = \frac{2.303\ A}{d} \quad (2)$$

Where, d denotes film thickness, A denotes absorbance, and T denotes transmittance.

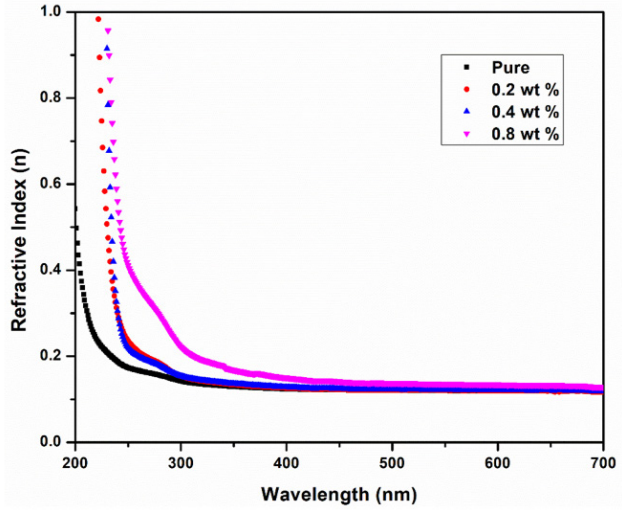

Figure 3: Refractive index (n) vs wavelength plot for pure and doped samples.

The absorption edge obtained from the absorption coefficient is used to classify the material [30]. The absorption edge is obtained by extrapolating the linear segment of the curves to zero absorption (α = 0). The pure film absorption edge (Ee) was 4.84 eV; however, it was reduced to 2.53 eV for 0.8 wt% NaBr films (shown in Table 1). The increase in intermolecular stacking and intramolecular charge transfer is responsible for the substantial change in the absorption edge in doped films [17].

Band gap study

The Tauc and Davis-Mott equation (3) [36] was used to assess the band gap of the samples.

$$\alpha = A(h\nu - E_g)^r \quad (3)$$

Where, E_g is optical energy bandgap, r is the exponent factor takes the values of ½, 2, 3/2 and 3 for direct and indirect allowed and forbidden electron excitations, respectively [37] (Figure 4).

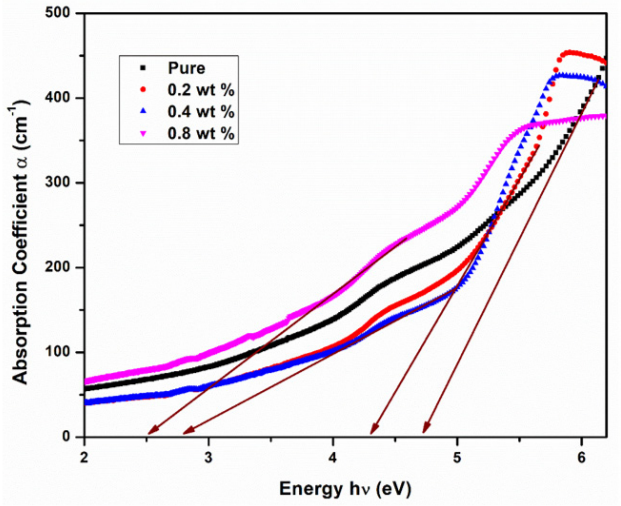

Figure 4: Absorption coefficient (α) vs photon energy of pure and doped samples.

The fluctuation of $(\alpha h\nu)^2$ and $(\alpha h\nu)^{1/2}$ as a function of the photon energy ($h\nu$) at ambient temperature is shown in figures 5 and 6, respectively. The linear area of curves may be connected to the shifts between the valence and conduction bands via the direct energy band gap (E_d) and indirect energy band gap (E_{ind}) transitions [38]. These values are calculated by extrapolating the linear section to zero absorption are shown in Table 1. The values E_d and E_{ind} fell from 5.59 to 2.57 eV and 4.61 to 2.44 eV, respectively. This illustrates that when the salt level increases, the samples become more semiconducting [39]. This would be due to an increase in the valence and conduction band shift. Furthermore, the existence of unsaturated defects enhances the density of localized states in the band gap, resulting in a decrease in the optical energy gap [40, 41].

Extinction coefficient (K)

The extinction coefficient (K) is the amount of light that is lost due to scattering and absorption per unit distance of penetrating medium. The increase in extinction coefficient with increasing photon energy shown in Figure 7 indicates that a fraction of light is reduced due to scattering and absorption increases. This is because absorption decreases at lower energy when the

Table 1: Absorption edge, direct bandgap, indirect bandgap, and estimated band gap at room temperature.

Sl. No.	HPMC/NaBr wt%	Absorption edge (E_e) eV	Direct bandgap (E_d) eV	Indirect bandgap (E_{ind}) eV
1.	Pure HPMC	4.84	5.59	4.61
2.	0.2	4.28	3.72	4.25
3.	0.4	2.75	3.44	2.64
4.	0.8	2.53	2.57	2.44

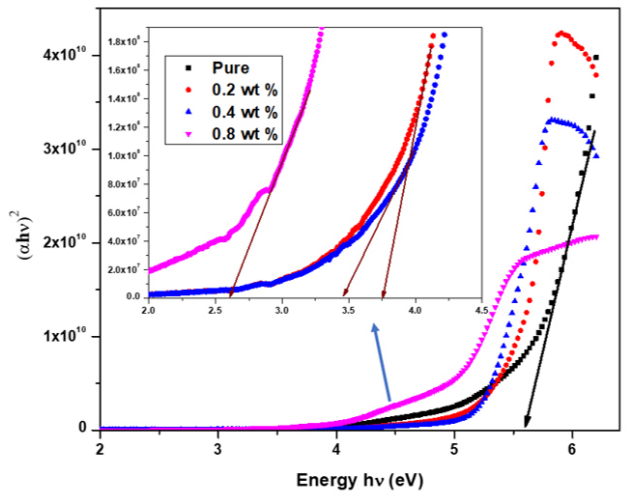

Figure 5: $(\alpha h\nu)^2$ vs photon energy (hν) of pure and doped samples.

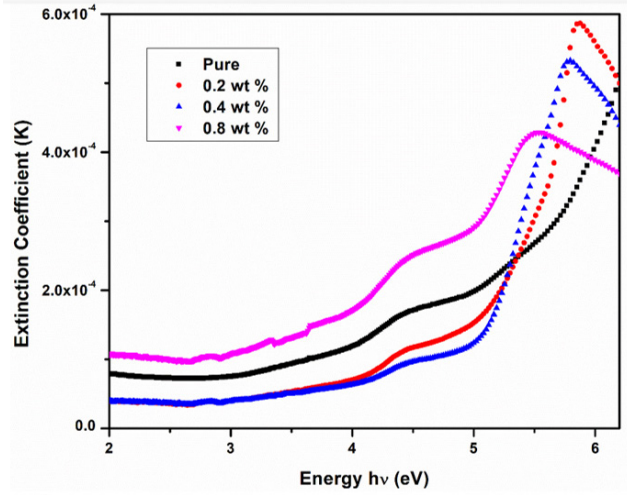

Figure 7: Extinction coefficient (K) vs photon energy (hν) of pure and doped samples.

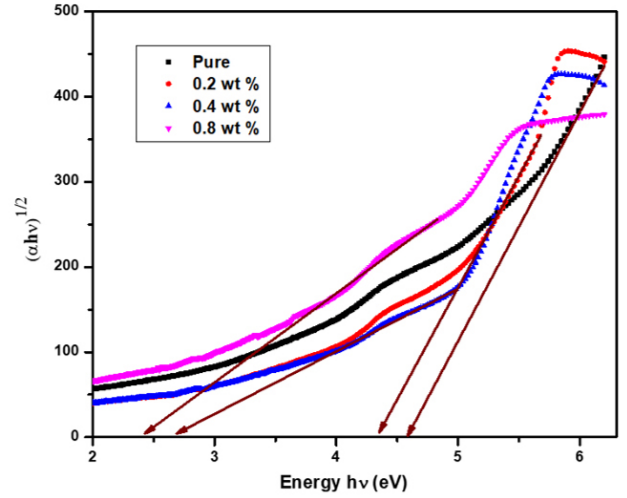

Figure 6: $(\alpha h\nu)^{1/2}$ vs photon energy ($h\nu$) for pure and doped samples.

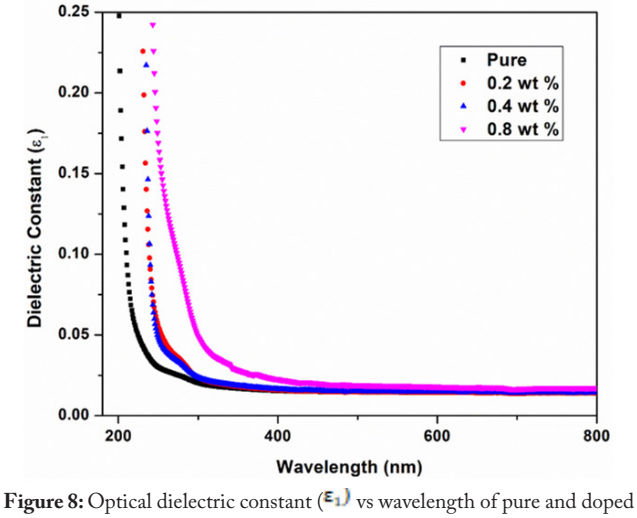

Figure 8: Optical dielectric constant (ε_1) vs wavelength of pure and doped samples.

falling photon energy is smaller than the energy gap [42].

$$K = \frac{\lambda\alpha}{4\pi} \qquad (4)$$

Optical dielectric function (ε*)

The dielectric function is highly dependent on the band structure of the material. The dielectric function is essential; the real component (ε_1) of the dielectric function relates to an electronic part, and the imaginary part (ε_2) pertains to the optical absorptions of the materials and has a direct correlation to the valence and conduction band [43]. Figure 8 depicts an optical dielectric constant (ε_1) vs. wavelength graph, with the vertex of the curve shifting towards the higher wavelength as salt content increases. The well-known Penn's model [44] is validated by the greatest value of the optical dielectric constant (ε_1) for the smallest optical band gap. Figure 9 depicts the optical dielectric loss as a function of photon energy. The absorption edge was shown to be reallocated to lower photon energy in doped films. It has been found that the dielectric loss absorption edge should be fairly comparable to Tauc's relation anticipated values [45]. Table 1 displays the band gap values computed using both methodologies (optical

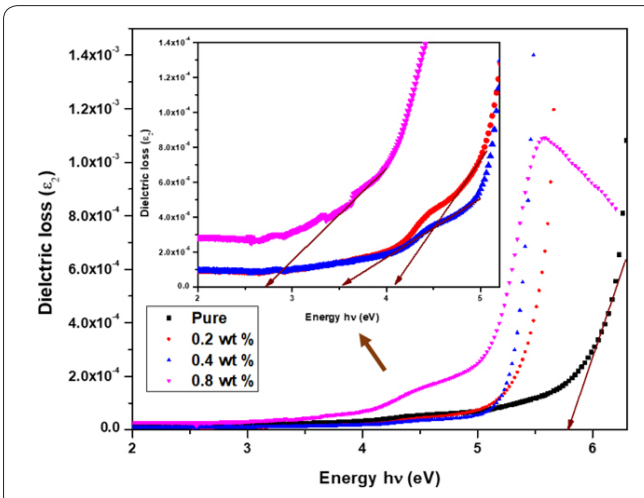

Figure 9: Optical dielectric loss (ε_2) vs photon energy (hν) of pure and doped samples.

dielectric loss and Tauc). Previous studies already have shown that Tauc's and optical dielectric loss models can be used to fix the mode of electronic transition and band gap respectively

[46, 47].

The real and imaginary components of the dielectric function can be calculated by equation (5) and (6)

$$\varepsilon_{1=} n^2 - K^2 \quad (5)$$

$$\varepsilon_{2=} 2nK \quad (6)$$

Optical conductivity (σopt)

One of the most important parameters that affect a material's optical properties is its optical conductivity σ_{opt}. It is used to highlight the material's allowable interband optical transitions. The relationship between optical conductivity and photon energy is displayed in Figure 10. Optical conductivity improves with photon energy. The rise in absorption coefficient is accountable for the excitation of carriers from the valence to the conduction band.

The optical conductivity (σ_{opt}) is given by equation (7) [48].

$$\sigma_{opt} = \frac{\alpha nc}{4\pi} \quad (7)$$

Where, α is the absorption coefficient, n is the refractive index and c is the velocity of light.

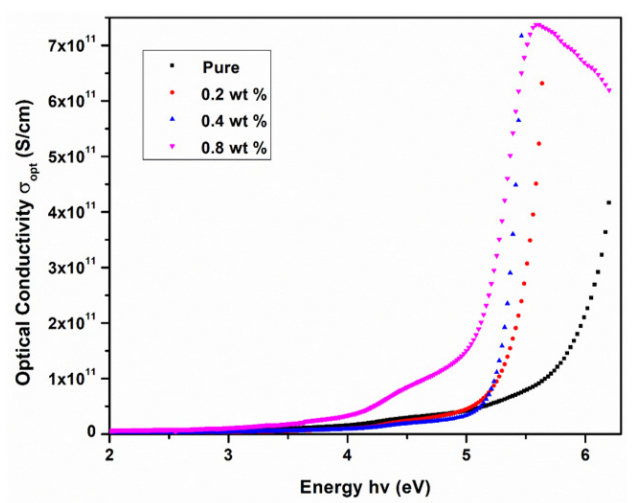

Figure 10: Optical conductivity vs photon energy (hν) of pure and doped samples.

XRD study

The XRD patterns of pure HPMC shows only two distinct peaks at 8° and 21° (Figure 10). Wang et al. reported comparable findings. who had created a hydrogel using chitosan, HPMC, and glycerol [49]. They also observed only two peaks at 7.9° and 20.3°. The intensity of the first peak almost vanished with salt concentration but the second broad peak broadened with the salt concentration this shows the decrease of the crystalline portion and increase of the amorphous portion which causes the reduction of the optical band gap. Similar outcomes were obtained by Nofal et al. who had prepared Co^{2+}-polyphenol with polyvinyl alcohol polymer to get desired optical parameters [50].

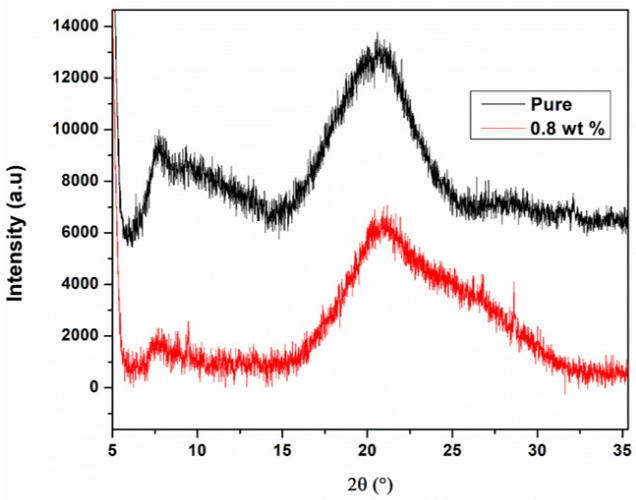

Figure 11: XRD of pure and doped samples.

Conclusion

The narrow bandgap solid polymer electrolyte films were successfully prepared by the solution casting method. The optical characteristics of the samples have been characterized. The optical absorption edge and optical energy gaps (indirect and direct) exhibit a significant decline as dopant salt concentration increases. On doping, these values moved to lower energies. This suggests that the doped HPMC films become semiconducting nature. This is owing to the significant population of carriers in the valence and conduction bands, which promotes carrier-carrier interaction and shifts the valence and conduction band. Also, the existence of unsaturated defects also aids in a reduction in the optical band gap. The optical band gap was precisely measured using the optical dielectric loss graph, and the nature of electronic transition was established using Tauc's method. The results of the highest optical dielectric constant for the shortest optical band gap obeyed Penn's model. The XRD measurements confirm the semicrystalline phase of HPMC and the amorphous area expanded with dopant concentration, which narrows the optical bandgap. The observed narrow bandgap demonstrates its potential for optoelectronic devices.

Acknowledgement

Sunil Kumar expresses gratitude to S. D. V. S. Sangh's S. S. Arts College and T. P. Science Institute for their financial support.

Conflict of Interest

The authors declare that they have no conflict of interest.

References

1. Asnawi A, Hamsan M, Aziz S, Kadir M, Matmin J, et al. 2021. Impregnation of [Emim] Br ionic liquid as plasticizer in biopolymer electrolytes for EDLC application. *Electrochim Acta* 375: 137923. https://doi.org/10.1016/j.electacta.2021.137923
2. Aziz S, Nofal M, Kadir M, Dannoun E, Brza M, et al. 2021. Bio-based plasticized PVA based polymer blend electrolytes for energy storage EDLC devices: ion transport parameters and electrochemical properties. *Materials* 14(8): 1994. https://doi.org/10.3390/ma14081994

3. Wang H, S Li, Yasin G, W Li, Xu H, et al. 2020. Reviewing the current status and development of polymer electrolytes for solid-state lithium batteries. *Energy Storage Mater* 33: 188-215. https://doi.org/10.1016/j.ensm.2020.08.014
4. Fenton DE, Parker JM, Wright PV. 1973. Complexes of alkali-metal ions with poly(ethylene oxide). *Polymer* 14(11): 589–589. https://doi.org/10.1016/0032-3861(73)90146-8
5. Vashishta P, Mundy JN, Shenoy GK. 1979. Fast ion transport in solids electrodes and electrolytes. Elsevier North Holland Inc, Lake Geneva, New York, USA.
6. El-Kader KMA, Orabi AS. 2002. Spectroscopic behavior of poly(vinyl alcohol) films with different molecular weights. *Polym Test* 21(5): 591–595. https://doi.org/10.1016/S0142-9418(01)00129-5
7. Hamad TK. 2013. Refractive index dispersion and analysis of the optical parameters of (PMMA/PVA) thin film. *Journal of Al-Nahrain University* 16(3): 164–170.
8. Li W, Hendriks KH, Wienk MM, Janssen RA. 2016. Diketopyrrolopyrrole polymers for organic solar cells. *Acc Chem Res* 49: 78–85. https://doi.org/10.1021/acs.accounts.5b00334
9. Meng D, Sun D, Zhong C, Liu T, Fan B, et al. 2016. High-performance solution-processed non-fullerene organic solar cells based on selenophene-containing perylene bisimide acceptor. *J Am Chem Soc* 138(1): 375–380. https://doi.org/10.1021/jacs.5b11149
10. Aziz SB, Abdullah OG, Hussein AM, Abdulwahid RT, Rasheed MA, et al. 2017. Optical properties of pure and doped PVA:PEO based solid polymer blend electrolytes: two methods for band gap study. *J Mater Sci: Mater Electron* 28: 7473–7479. https://doi.org/10.1007/s10854-017-6437-1
11. Abdullah OG, Aziz SB, Rasheed MA. 2016. Structural and optical characterization of PVA:$KMnO_4$ based solid polymer electrolyte. *Results Phys* 6: 1103-1108. https://doi.org/10.1016/j.rinp.2016.11.050
12. Badry R, El-Khodary S, Elhaes H, Nada N, Ibrahim M. 2021. Optical, conductivity and dielectric properties of plasticized solid polymer electrolytes based on blends of sodium carboxymethyl cellulose and polyethylene oxide. *Opt Quant Electron* 53: 3. https://doi.org/10.1007/s11082-020-02649-2
13. Wu Y, Wadia C, Ma W, Sadtler B, Alivisatos AP. 2008. Synthesis and photovoltaic application of copper(I) sulfide nanocrystals. *Nano Lett* 8(8): 2551–2555. https://doi.org/10.1021/nl801817d
14. Ito S, Hirose A, Yamaguchi M, Tanaka K, Chujo Y. 2017. Synthesis of aggregation-induced emission-active conjugated polymers composed of group 13 diiminate complexes with tunable energy levels via alteration of central element. *Polymers* 9(2): 68. https://doi.org/10.3390/polym9020068
15. Mallajosyula AT, Srivastava N, Iyer SSK, Mazhari B. 2010. Characterization of matrix and isolated organic solar cells. Sol *Energy Mater Sol Cells* 94(8): 1319–1323. https://doi.org/10.1016/j.solmat.2008.09.027
16. Ryusuke T, Maurer R, Jacob L, Stowasser F, Stillhart C, et al. 2020. Formulating amorphous solid dispersions: impact of inorganic salts on drug release from tablets containing itraconazole-HPMC extrudate. *Mol Pharmaceutics* 17(8): 2768-2778. https://doi.org/10.1021/acs.molpharmaceut.9b01109
17. Kumar S, Demappa T, Sannappa J. 2022. Influence of KI salt concentration on the hydroxypropyl methylcellulose films: optical study. *Opt Mater* 129: 112474. https://doi.org/10.1016/j.optmat.2022.112474
18. Kim H, Kim H, Ding Z, Lee MH, Lim K, et al. 2016. Recent progress in electrode materials for sodium-ion batteries. *Adv Energy Mater* 6(19): 1600943. https://doi.org/10.1002/aenm.201600943
19. Kim SM, Seo DH, Ma X, Ceder G, Kang K. 2012. Electrode materials for rechargeable sodium-ion batteries: potential alternatives to current lithium-ion batteries. *Adv Energy Mater* 2(7): 710-721. https://doi.org/10.1002/aenm.201200026
20. Yabuuchi N, Kubota K, Dahbi M, Komaba S. 2014. Research development on sodium-ion batteries. *Chem Rev* 114(23): 11636-11682. https://doi.org/10.1021/cr500192f
21. Fuentes I, Andrio A, Teixidor F, Viñas C, Compañ V. 2017. Enhanced conductivity of sodium versus lithium salts measured by impedance spectroscopy. Sodium cobaltacarboranes as electrolytes of choice. *Phys Chem Chem Phys* 19(23): 15177–15186. https://doi.org/10.1039/C7CP02526B
22. Pan H, Hu YS, Chen L. 2013. Room-temperature stationary sodium-ion batteries for large-scale electric energy storage. *Energy Environ Sci* 6: 2338-2360. https://doi.org/10.1039/C3EE40847G
23. Bella F, Colò F, Nair JR, Gerbaldi C. 2015. Photopolymer electrolytes for sustainable, upscalable, safe, and ambient-temperature sodium-ion secondary batteries. *Chem Sus Chem* 8(21): 3668-3676. https://doi.org/10.1002/cssc.201500873
24. Rao BL, Shivananda CS, Shetty GR, Harish KV, Madhukumar R, et al. 2018. Influence of UV irradiation on hydroxypropyl methyl cellulose polymer films. *AIP conference proceedings* pp 080011. https://doi.org/10.1063/1.5032817
25. Chen Z, Zheng Y, Yan H, Facchetti A. 2009. Naphthalenedicarboximide- vs perylene dicarboximide-based copolymers. Synthesis and semiconducting properties in bottom-gate n-channel organic transistors. *J Am Chem Soc* 131(1): 8-9. https://doi.org/10.1021/ja805407g
26. Ahmed E, Ren G, Kim FS, Hollenbeck EC, Jenekhe SA. 2011. Design of new electron acceptor materials for organic photovoltaics: synthesis, electron transport, photophysics, and photovoltaic properties of oligothiophene-functionalized naphthalene diimides. *Chem Mater* 23(20): 4563–4577. https://doi.org/10.1021/cm2019668
27. Al-Taa'y WA, Abdul Nabi MT, Al-Rawi TK. 2011. The MR affect on optical properties for poly (vinyl alcohol) films. *Baghdad Sci J* 8(2): 543–550.
28. Lobo B, Ranganath MR, Chandran TR, Rao GV, Ravindrachary V, et al. 1999. Iodine-doped polyvinyl alcohol using positron annihilation spectroscopy. *Phys Rev B* 59(21): 13693–13698. https://doi.org/10.1103/PhysRevB.59.13693
29. El-Deen HZ, Hafez AI. 2009. Physico-chemical stability of PVA films doped with Mn^{2+} ions against weathering conditions. *Arab J Sci Eng* 34(1A): 13–26.
30. Guirguis OW, Moselhey MT. 2011. Optical study of poly (vinyl alcohol)/hydroxypropyl methylcellulose blends. *J Mater Sci* 46: 5775–5789. https://doi.org/10.1007/s10853-011-5533-5
31. Sanderson GR. 1981. Polysaccharides in foods. *Food Technol* 35(7): 50–57.
32. Aziz SB, Abdulwahid RT, Rsaul RA, Ahmed HM. 2016. *In situ* synthesis of CuS nanoparticle with a distinguishable SPR peak in NIR region. *J Mater Sci Mater Electron* 27: 4163–4171. https://doi.org/10.1007/s10854-016-4278-y
33. Ditta MA, Farrukh MA, Ali S, Younas N. 2017. X-ray peak profiling, optical parameters and catalytic properties of pure and CdS doped ZnO–NiO nanocomposites. *Russ J Appl Chem* 90(1): 151–159. https://doi.org/10.1134/S1070427217010220
34. Sharma P, Katyal SC. 2007. Determination of optical parameters of a-$(As_2Se_3)90Ge_{10}$ thin film. *J Phys D Appl Phys* 40(7): 2115. https://doi.org/10.1088/0022-3727/40/7/038
35. Juma AO, Arbab EA, Muiva CM, Lepodise LM, Mola GT. 2017. Synthesis and characterization of CuO-NiO-ZnO mixed metal oxide nanocomposite. *J Alloy Comp* 723: 866-872. https://doi.org/10.1016/j.jallcom.2017.06.288
36. Bakr NA, Funde AM, Waman VS, Kamble MM, Hawaldar RR, et al. 2011. Determination of the optical parameters of a-Si:H thin films deposited by hot wire-chemical vapour deposition technique using transmission spectrum only. *Pramana - J Phys* 76: 519–531. https://doi.org/10.1007/s12043-011-0024-4

37. Ibrahim S, Ahmad R, Johan MR. 2012. Conductivity and optical studies of plasticized solid polymer electrolytes doped with carbon nanotube. *J Lumin* 132(1): 147–152. https://doi.org/10.1016/j.jlumin.2011.08.004

38. Kumar GV, Chandramani R. 2009. Investigations on Fe^{3+} doped polyvinyl alcohol films with and without gamma (γ)-irradiation. *App Surfac Sci* 255(15): 7047–7050. https://doi.org/10.1016/j.apsusc.2009.03.038

39. Siddaiah T, Ojha P, Gopal NO, Ramu C, Nagabhushana H. 2018. Thermal, structural, optical and electrical properties of PVA/MAA:EA polymer blend filled with different concentrations of lithium perchlorate. *J Sci Adv Mater Devices* 3(4): 456–63. https://doi.org/10.1016/j.jsamd.2018.11.004

40. Bhunia R, Ghosh D, Ghosh B, Hussain S, Bhar R, et al. 2015. Free-standing flexible nanocrystalline-ZnO-impregnated polyvinylidene fluoride composite thin films. *J Compos Mater* 49(25): 3089-3101. https://doi.org/10.1177/0021998314559756

41. Sheela T, Bhajantri RF, Ravindrachary V, Rathod SG, Pujari PK, et al. 2014. Effect of UV irradiation on optical, mechanical and microstructural properties of PVA/NaAlg blends. *Rad Phys Chem* 103: 45–52. https://doi.org/10.1016/j.radphyschem.2014.05.036

42. Nadeem MY, Ahmed W. 2000. Optical properties of ZnS thin films. *Turk J Phys* 24(5): 651-659.

43. Biskri ZE, Rached H, Bouchear M, Rached D, Aida MS. 2016. A comparative study of structural stability and mechanical and optical properties of fluorapatite ($Ca_5(PO_4)_3F$) and lithium disilicate ($Li_2Si_2O_5$) components forming dental glass–ceramics: first principles study. *J Electron Mater* 45: 5082–5095. https://doi.org/10.1007/s11664-016-4681-4

44. Ravindra NM, Ganapathy P, Choi J. 2007. Energy gap–refractive index relations in semiconductors-an overview. *Infrared Phys Technol* 50(1): 21–29. https://doi.org/10.1016/j.infrared.2006.04.001

45. Yu L, Li D, Zhao S, Li G, Yang K. 2012. First principles study on electronic structure and optical properties of ternary GaAs:Bi alloy. *Materials* 5(12): 2486–2497. https://doi.org/10.3390/ma5122486

46. Aziz SB, Ahmed HM, Hussein AM, Fathulla AB, Wsw RM, et al. 2015. Tuning the absorption of ultraviolet spectra and optical parameters of aluminium doped PVA based solid polymer composites. *J Mater Sci Mater Electron* 26: 8022–8028. https://doi.org/10.1007/s10854-015-3457-6

47. Aziz SB. 2016. Modifying poly(vinyl alcohol) (PVA) from insulator to smallband gap polymer: a novel approach for organic solar cells and optoelectronic devices. *J Electron Mater* 45: 736–745. https://doi.org/10.1007/s11664-015-4191-9

48. Yakuphanoglu F, Cukurovali A, Yilmaz I. 2005. Refractive index and optical absorption properties of the complexes of a cyclobutane containing thiazolyl hydrazone ligand. *Opt Mater* 27(8): 1363–1368. https://doi.org/10.1016/j.optmat.2004.09.021

49. Wang T, Chen L, Shen T, Wu D. 2016. Preparation and properties of a novel thermo-sensitive hydrogel based on chitosan/hydroxypropyl methylcellulose/glycerol. *Int J Biol Macromol* 93: 775–782. https://doi.org/10.1016/j.ijbiomac.2016.09.038

50. Nofal MM, Aziz SB, Hadi JM, Karim WO, Dannoun EM et al. 2021. Polymer composites with 0.98 transparencies and small optical energy band gap using a promising green methodology: structural and optical properties. *Polymers* 13(10): 1648. https://doi.org/10.3390/polym13101648